
On Calibration of Ensemble-Based Credal Predictors

Thomas Mortier

Dept. of Data Analysis and Mathematical Modelling
Ghent University
Coupure links 653, Ghent, Belgium

Viktor Bengs

Institute of Informatics
LMU Munich
Akademiestr. 7, Munich, Germany

Eyke Hüllermeier

Institute of Informatics
LMU Munich
Akademiestr. 7, Munich, Germany

Stijn Luca

Dept. of Data Analysis and Mathematical Modelling
Ghent University
Coupure links 653, Ghent, Belgium

Willem Waegeman

Dept. of Data Analysis and Mathematical Modelling
Ghent University
Coupure links 653, Ghent, Belgium

Abstract

In recent years, several classification methods that intend to quantify epistemic uncertainty have been proposed, either by producing predictions in the form of second-order distributions or sets of probability distributions. In this work, we focus on the latter, also called credal predictors, and address the question of how to evaluate them: What does it mean that a credal predictor represents epistemic uncertainty in a faithful manner? To answer this question, we refer to the notion of calibration of probabilistic predictors and extend it to credal predictors. Broadly speaking, we call a credal predictor calibrated if it returns sets that cover the true conditional probability distribution. To verify this property for the important case of ensemble-based credal predictors, we propose a novel nonparametric calibration test that generalizes an existing test for probabilistic predictors to the case of credal predictors. Making use of this test, we empirically show that credal predictors based on deep neural networks are often not well calibrated.

1 Introduction

There is a general consensus that trustworthy machine learning systems should not only return accurate predictions, but also a credible representation of their uncertainty. In this regard, two inherently different sources of uncertainty are often distinguished, referred to as *aleatoric* and *epistemic* [Hora, 1996], and various methods that quantify these types of uncertainty have been proposed [Senge et al., 2014, Kendall and Gal, 2017, Hüllermeier and Waegeman, 2021]. Most methods focus on *predictive uncertainty*, i.e., the learner’s uncertainty in the outcome $y \in \mathcal{Y}$ given a query instance $\mathbf{x} \in \mathcal{X}$ for which a prediction is sought. The aleatoric part of this uncertainty corresponds to uncertainty that cannot be reduced by further information (e.g., more training data), as it originates from wrong class annotations or a lack of informative features. Therefore, the “ground-truth” is a conditional probability distribution $p(\cdot | \mathbf{x})$ on \mathcal{Y} , i.e., each outcome y has a certain probability $p(y | \mathbf{x})$ to occur. Even with perfect knowledge about the underlying data-generating process, the outcome cannot be predicted with certainty.

In a typical machine learning scenario, the learner does not know $p(\cdot | \mathbf{x})$. Instead, it uses an estimate $\hat{p}(\cdot | \mathbf{x})$ based on the training data as a surrogate. In essence, epistemic uncertainty refers to the uncertainty about the true p , or the “gap” between p and \hat{p} . Methods that represent this (second-order) uncertainty typically do not return a single $\hat{p}(\cdot | \mathbf{x})$, but either a distribution over $\hat{p}(\cdot | \mathbf{x})$, or sets containing different $\hat{p}(\cdot | \mathbf{x})$. Distributions over $\hat{p}(\cdot | \mathbf{x})$ are obtained for Bayesian methods such as Gaussian processes and Bayesian neural networks [Depeweg et al., 2018], as well as in methods that optimize the parameters of Dirichlet or normal-inverse Gamma distributions via tailored loss functions [Sensoy et al., 2018b, Malinin and Gales, 2018, Charpentier et al., 2020, Amini et al., 2020]. Sets containing different $\hat{p}(\cdot | \mathbf{x})$ appear in various types of ensemble methods, such as random forests [Shaker and Hüllermeier, 2020], deep ensembles [Lakshminarayanan et al., 2017], and dropout networks [Gal, 2016], as well as in the literature on so-called credal predictors [Corani and Antonucci, 2014, Yang et al., 2014].

Without any doubt, quantifying epistemic uncertainty in an objective way is far from trivial, and so is the evaluation of such quantifications. For lack of an objective ground-truth, most methods evaluate epistemic uncertainty representations in an indirect manner, using downstream tasks such as out-of-distribution detection [Ovadia et al., 2019], robustness to adversarial attacks [Kopetzki et al., 2021] or active learning [Nguyen et al., 2022]. However, all those tasks are characterized by a scenario where training and test data are not identically distributed. Therefore, several recent studies have raised concerns about the usefulness of such tasks w.r.t. epistemic uncertainty evaluation. Many of the above-mentioned methods typically perform very well in experimental studies where training and test data are not identically distributed, but those methods also have obvious limitations w.r.t. uncertainty quantification. For example, some very recent papers discuss crucial limitations of deep ensembles [Abe et al., 2022], dropout networks [Dewolf et al., 2021], and methods that fit the parameters of Dirichlet distributions [Bengts et al., 2022].

We argue that epistemic uncertainty estimation is also important when training and test data are identically distributed, and we propose a novel procedure to evaluate epistemic uncertainty representations in a more direct way. To this end, we focus on the multi-class classification setting, where aleatoric uncertainty representations are typically evaluated using calibration tests for a single estimated model $\hat{p}(\cdot | \mathbf{x})$, see e.g. [Hosmer and Lemeshow, 2003, Vaicenavicius et al., 2019, Widmann et al., 2019]. For the first time, we present a calibration test for epistemic uncertainty representations in the form of credal sets, i.e., set of probability distributions (the situation where distributions over $\hat{p}(\cdot | \mathbf{x})$ are considered is left for future work). Technically, since all members in a credal set need to be tested, a problem of multiple hypothesis testing arises, and a resampling approach that bounds the Type I error is presented. In the experiments we perform simulations to analyze the Type I and Type II error for various calibration measures and conditions. Lastly, we apply the newly-developed test to analyze whether deep ensembles and dropout networks represent epistemic uncertainty in a correct manner.

2 Aleatoric Uncertainty Evaluation

In this section we formally review existing calibration tests for multi-class classification problems. With such tests, aleatoric uncertainty representations of classifiers can be evaluated in a natural and direct way. In the following section, these tests will be extended for epistemic uncertainty representations in the form of credal sets. This section can hence be interpreted as a discussion of closely-related work, but it also intends to introduce the mathematical concepts needed further on.

2.1 Different notions of calibration

Consider a standard multi-class classification setting with instance space \mathcal{X} and label space $\mathcal{Y} = \{1, \dots, K\}$. We assume that the data is i.i.d. according to an underlying joint probability measure P on $\mathcal{X} \times \mathcal{Y}$. Correspondingly, each instance $\mathbf{x} \in \mathcal{X}$ is associated with a conditional distribution $p(Y | \mathbf{x})$ on \mathcal{Y} , such that $p(Y = k | \mathbf{x})$ is the probability to observe class k as an outcome given \mathbf{x} . For a hypothesis space \mathcal{H} , a probabilistic predictor $\hat{p} \in \mathcal{H}$ can then be defined as a mapping $\hat{p} : \mathcal{X} \rightarrow \Delta_K$, where Δ_K denotes the $(K - 1)$ -simplex

$$\Delta_K := \{\boldsymbol{\theta} = (\theta_1, \dots, \theta_K) \in [0, 1]^K \mid \|\boldsymbol{\theta}\|_1 = 1\} \quad (1)$$

of probability vectors $\boldsymbol{\theta}$, each of which identifies a categorical distribution $\text{Cat}(\boldsymbol{\theta})$. Let us remark that we will utilize bold lowercase letters for vectors and vector functions, e.g., $\boldsymbol{\theta}$ and $\hat{\boldsymbol{p}}(\boldsymbol{x})$, whereas a normal font will depict the components of these vectors, e.g., θ_k and $\hat{p}_k(\boldsymbol{x})$.

We start by formally defining confidence calibration [Guo et al., 2017]. This notion of calibration is by far the most often used in literature [Filho et al., 2021]. Let's assume that we have fitted a probabilistic predictor that estimates $p(Y|\boldsymbol{x})$, leading to the estimate $\hat{\boldsymbol{p}}(\boldsymbol{x})$. Furthermore, let $c(\boldsymbol{x}) = \max_k \hat{p}_k(\boldsymbol{x})$ be the mode of the estimated conditional class distribution for instance \boldsymbol{x} (or confidence score) and let $f(\boldsymbol{x}) = \operatorname{argmax}_k \hat{p}_k(\boldsymbol{x})$ be the corresponding prediction.

Definition 1. A multi-class classifier is confidence calibrated if it holds that

$$\mathbb{P}_{(\boldsymbol{X}, Y) \sim P} (Y = f(\boldsymbol{X}) | c(\boldsymbol{X}) = s) = s.$$

This is a rather weak notion of calibration, as only the mode of the conditional distribution needs to be calibrated. A stronger form of calibration is classwise calibration [Zadrozny and Elkan, 2001].

Definition 2. A multi-class classifier is classwise calibrated if for all $k \in \{1, \dots, K\}$ it holds that

$$\mathbb{P}_{(\boldsymbol{X}, Y) \sim P} (Y = k | \hat{p}_k(\boldsymbol{X}) = s) = s.$$

A few authors define an even stronger notion of calibration, sometimes referred to as calibration in the strong sense [Widmann et al., 2019, Filho et al., 2021].

Definition 3. A multi-class classifier is calibrated in the strong sense if for all $k \in \{1, \dots, K\}$ it holds that

$$\mathbb{P}_{(\boldsymbol{X}, Y) \sim P} (Y = k | \hat{\boldsymbol{p}}(\boldsymbol{X}) = \boldsymbol{s}) = s_k,$$

with s_k the k -th component of \boldsymbol{s} .

2.2 Calibration tests

All three definitions of calibration assume that one knows the true underlying distribution P . However, in practice, this distribution is unknown, so one needs to replace the expectation by a finite-sample estimate. In addition, a calibration measure that quantifies the discrepancy between observed and expected frequencies is needed. In a final step, this calibration measure can be used to construct a statistical test that decides whether a multi-class classifier is calibrated or not. In the literature, three different types of tests have been developed. The Hosmer-Lemeshow test is a specific type of chi-squared test that is commonly used as a goodness-of-fit test for logistic and multinomial regression models in statistics [Hosmer and Lemeshow, 2003, Fagerland et al., 2008]. The resampling-based test of Vaicenavicius et al. [2019] and the kernel-based test of Widmann et al. [2019] have been proposed more recently in the machine learning literature. The Hosmer-Lemeshow test can only be used to assess classwise calibration, whereas the other tests are more general, because they can be used in combination with a wide range of calibration measures. All tests analyze the null hypothesis H_0 : $\hat{\boldsymbol{p}}$ is calibrated versus the alternative H_1 : $\hat{\boldsymbol{p}}$ is not calibrated, where the notion of calibration (i.e., confidence, classwise or strong) depends on the underlying test.

We first explain formally the Hosmer-Lemeshow test, originally proposed for binary logistic regression, and later extended to the more general class of multinomial probabilistic models [Fagerland et al., 2008]. Let $\mathcal{D}_{val} = \{(\boldsymbol{x}_1, y_1), \dots, (\boldsymbol{x}_N, y_N)\}$ be a validation set of size N , i.i.d. according to P . We will use the shorthand notation \hat{p}_{ik} for the estimated probability $\hat{p}_k(\boldsymbol{x}_i)$. Let $c_i = \operatorname{argmax}_k \hat{p}_{ik}$ be the highest probability for instance \boldsymbol{x}_i and let $\hat{y}_i = \operatorname{argmax}_k \hat{p}_{ik}$ be the predicted label. For every label y_i , let us consider a K -dimensional vector \boldsymbol{y}_i that defines the one-hot encoding of y_i , i.e., $y_{ik} = 1$ iff $y_i = k$. Similarly as for the true label, we transform \hat{y}_i to a K -dimensional vector $\hat{\boldsymbol{y}}_i$ that defines the one-hot encoding of \hat{y}_i , i.e., $\hat{y}_{ik} = 1$ iff $\hat{y}_i = k$.

For class k , the probabilities $\hat{p}_{1k}, \dots, \hat{p}_{Nk}$ are sorted, and the corresponding instances are placed into equal-frequency bins $\mathcal{B}_{1k}, \dots, \mathcal{B}_{Bk}$ with B the number of bins. Furthermore, the following test statistic is considered:

$$HL_{classwise}(\hat{\boldsymbol{p}}, \mathcal{D}_{val}) = \sum_{k=1}^K \sum_{j=1}^B \frac{(o(\mathcal{B}_{jk}) - p(\mathcal{B}_{jk}))^2}{p(\mathcal{B}_{jk})}, \quad (2)$$

where $o(\mathcal{B}_{jk})$ and $p(\mathcal{B}_{jk})$ denote the observed and expected probabilities in bin \mathcal{B}_{jk} , respectively:

$$o(\mathcal{B}_{jk}) = \frac{1}{|\mathcal{B}_{jk}|} \sum_{i: \hat{p}_{ik} \in \mathcal{B}_{jk}} y_{ik}, \quad \text{and} \quad p(\mathcal{B}_{jk}) = \frac{1}{|\mathcal{B}_{jk}|} \sum_{i: \hat{p}_{ik} \in \mathcal{B}_{jk}} \hat{p}_{ik}. \quad (3)$$

Fagerland et al. [2008] argued that (2) follows a chi-squared distribution with $(K - 1)(B - 2)$ degrees of freedom, and they derived p-values using this assumption. Let us remark that, besides the Hosmer-Lemeshow test, many other alternative goodness-of-fit tests exist in statistics, but these usually do not assess model calibration in a direct manner.

Vaicenavicius et al. [2019] developed a more general (nonparametric) test that can be adopted to assess confidence calibration, classwise calibration and calibration in the strong sense, depending on the calibration measure that is used. This test constructs a bootstrap distribution of any calibration measure empirically, under the null hypothesis that a classifier is calibrated, by resampling new labels multiple times from the probabilistic model that is under assessment. After constructing the distribution of the calibration measure under the null hypothesis, the test verifies, for the observed labels, how likely the calibration measure is under the assumption of a calibrated model.

The test of Vaicenavicius et al. [2019] is often used with the expected calibration error (ECE) as calibration measure. This measure has been originally introduced for binary problems as a way to evaluate reliability diagrams in a quantitative manner. The classwise extension of this measure in fact looks very similar to the Hosmer-Lemeshow test statistic:

$$ECE_{cwise}(\hat{\mathbf{p}}, \mathcal{D}_{val}) = \frac{1}{K} \sum_{k=1}^K \sum_{j=1}^B \frac{|\mathcal{B}_{jk}|}{N} |o(\mathcal{B}_{jk}) - p(\mathcal{B}_{jk})|, \quad (4)$$

with $o(\mathcal{B}_{jk})$ and $p(\mathcal{B}_{jk})$ as in (3). However, for the expected calibration error, the $[0, 1]$ -interval is often subdivided in intervals of equal length instead of equal frequency, i.e., $\mathcal{B}_{jk} := \{i : \frac{j-1}{B} \leq \hat{p}_{ik} < \frac{j}{B}\}$.

For the confidence-based extension of expected calibration error, binning only has to be done once (so, not for every class k). Let us divide the unit interval into B subintervals of equal length. With the j -th subinterval we associate the bin $\mathcal{B}_j := \{i : \frac{j-1}{B} \leq c_i < \frac{j}{B}\}$. Then, the calibration measure becomes:

$$ECE_{conf}(\hat{\mathbf{p}}, \mathcal{D}_{val}) = \sum_{j=1}^B \frac{|\mathcal{B}_j|}{N} |\text{Acc}(\mathcal{B}_j) - c(\mathcal{B}_j)|, \quad (5)$$

with

$$\text{Acc}(\mathcal{B}_j) = \frac{1}{|\mathcal{B}_j|} \sum_{i: c_i \in \mathcal{B}_j} \sum_{k=1}^K y_{ik} \hat{y}_{ik} \quad \text{and} \quad c(\mathcal{B}_j) = \frac{1}{|\mathcal{B}_j|} \sum_{i: c_i \in \mathcal{B}_j} c_i.$$

To test calibration in the strong sense, a different type of measure that is not based on binning is needed. Widmann et al. [2019] proposed a class of measures derived from matrix-valued kernel functions. For example, if one analyses all pairs of instances, while using a general matrix-valued kernel $\Gamma : \Delta_K \times \Delta_K \rightarrow \mathbb{R}^{K \times K}$, then the measure becomes:

$$\widehat{SKCE}_{uq}(\hat{\mathbf{p}}, \mathcal{D}_{val}) = \binom{N}{2}^{-1} \sum_{i=1}^{N-1} \sum_{j=i+1}^N \sum_{s=1}^K \sum_{t=1}^K (\hat{p}_{is} - y_{is})(\hat{p}_{jt} - y_{jt}) \Gamma_{st}(\hat{\mathbf{p}}(\mathbf{x}_i), \hat{\mathbf{p}}(\mathbf{x}_j)). \quad (6)$$

However, it is clear that calculating the above measure is computationally expensive when the number of instances N increases. For that reason, a similar estimator was proposed by the same authors:

$$\widehat{SKCE}_{ul}(\hat{\mathbf{p}}, \mathcal{D}_{val}) = \frac{1}{\lfloor N/2 \rfloor} \sum_{i=1}^{\lfloor N/2 \rfloor} \sum_{s,t=1}^K (\hat{p}_{(2i-1)s} - y_{(2i-1)s})(\hat{p}_{2it} - y_{2it}) \Gamma_{st}(\hat{\mathbf{p}}(\mathbf{x}_{2i-1}), \hat{\mathbf{p}}(\mathbf{x}_{2i})), \quad (7)$$

which is linear in N . Widmann et al. [2019] also consider other calibration measures, and they derive bounds and approximations on the p-value for the null hypothesis H_0 that the model is calibrated. These tests require a lot of space to explain, so we refer to the original paper for a further discussion.

3 Epistemic Uncertainty Evaluation

In this section we develop calibration tests for epistemic uncertainty representations, starting from the methodology that was reviewed in the previous section. As mentioned in the introduction, we will focus on the case where epistemic uncertainty is represented using credal sets, constructed from an ensemble of classifiers. In a typical ensemble learning scenario, one can assume that in total M different probabilistic models are fitted to the training data, denoted as $\mathcal{P} = \{\hat{\mathbf{p}}^{(1)}, \dots, \hat{\mathbf{p}}^{(M)}\}$, where $\hat{\mathbf{p}}^{(m)}$ represents the m -th model. We are interested in finding a convex combination of these M models, which leads to the creation of a convex set of distributions:

$$\mathcal{S}(\mathbf{x}, \mathcal{P}) = \left\{ \hat{\mathbf{p}}_{\boldsymbol{\lambda}}(\mathbf{x}) \in \mathcal{H} \mid \hat{\mathbf{p}}_{\boldsymbol{\lambda}}(\mathbf{x}) = \sum_{m=1}^M \lambda_m \hat{\mathbf{p}}^{(m)}(\mathbf{x}) \right\}, \quad (8)$$

where $\lambda_1, \dots, \lambda_M$ take values in the $(M - 1)$ -dimensional simplex:

$$\Delta_M := \left\{ \boldsymbol{\lambda} = (\lambda_1, \dots, \lambda_M) \in [0, 1]^M \mid \|\boldsymbol{\lambda}\|_1 = 1 \right\}. \quad (9)$$

The set of probability distributions $\mathcal{S}(\mathbf{x}, \mathcal{P})$ is referred to as a credal set, and is typically assumed to be convex and closed [Walley, 1991]. A credal set represents epistemic uncertainty, i.e., due to a limited training dataset, one cannot estimate the ground-truth probability distribution precisely, but this distribution should be contained in the credal set. An interpretation of that kind allows us to present natural extensions of confidence calibration, classwise calibration, and calibration in the strong sense for credal sets.

Definition 4. A credal set $\mathcal{S}(\mathbf{x}, \mathcal{P})$ is confidence calibrated if there exists a probabilistic model $\hat{\mathbf{p}}_{\boldsymbol{\lambda}}(\mathbf{x}) \in \mathcal{S}(\mathbf{x}, \mathcal{P})$, with corresponding confidence score $c_{\boldsymbol{\lambda}}(\mathbf{x})$ and mode $f_{\boldsymbol{\lambda}}(\mathbf{x})$, such that

$$\mathbb{P}_{(\mathbf{X}, Y) \sim P} (Y = f_{\boldsymbol{\lambda}}(\mathbf{X}) \mid c_{\boldsymbol{\lambda}}(\mathbf{X}) = s) = s.$$

$\mathcal{S}(\mathbf{x}, \mathcal{P})$ is classwise calibrated if there exists a probabilistic model $\hat{\mathbf{p}}_{\boldsymbol{\lambda}}(\mathbf{x}) \in \mathcal{S}(\mathbf{x}, \mathcal{P})$ such that, for all $k \in \{1, \dots, K\}$, it holds that

$$\mathbb{P}_{(\mathbf{X}, Y) \sim P} (Y = k \mid \hat{\mathbf{p}}_{\boldsymbol{\lambda}, k}(\mathbf{X}) = s) = s.$$

$\mathcal{S}(\mathbf{x}, \mathcal{P})$ is calibrated in the strong sense if there exists a probabilistic model $\hat{\mathbf{p}}_{\boldsymbol{\lambda}}(\mathbf{x}) \in \mathcal{S}(\mathbf{x}, \mathcal{P})$ such that, for all $k \in \{1, \dots, K\}$, it holds that

$$\mathbb{P}_{(\mathbf{X}, Y) \sim P} (Y = k \mid \hat{\mathbf{p}}_{\boldsymbol{\lambda}}(\mathbf{X}) = \mathbf{s}) = s_k.$$

In what follows, we develop a statistical test to verify whether a credal set is calibrated according to Def. 4, which translates to the following set of hypotheses:

$$H_0 : \mathcal{S}(\mathbf{x}, \mathcal{P}) \text{ is calibrated} \quad \text{vs.} \quad H_1 : \mathcal{S}(\mathbf{x}, \mathcal{P}) \text{ is not calibrated} \quad (10)$$

The above set of hypotheses can also be written as:

$$H_0 : \exists \boldsymbol{\lambda} \in \Delta_M \text{ s.t. } \hat{\mathbf{p}}_{\boldsymbol{\lambda}} \text{ is calibrated} \quad \text{vs.} \quad H_1 : \forall \boldsymbol{\lambda} \in \Delta_M \text{ it holds that } \hat{\mathbf{p}}_{\boldsymbol{\lambda}} \text{ is not calibrated} \quad (11)$$

While the test problem in (10) focuses on the question whether a *single* fixed probabilistic classifier $\hat{\mathbf{p}}$ is calibrated, the test problem in (11) asks for the existence of a calibrated convex combination of the finite set of probabilistic classifiers. Thus, the latter is essentially a multiple comparison problem, as we simultaneously test the hypotheses

$$H_{0, \boldsymbol{\lambda}} : \hat{\mathbf{p}}_{\boldsymbol{\lambda}} \text{ is calibrated} \quad \text{vs.} \quad H_{1, \boldsymbol{\lambda}} : \hat{\mathbf{p}}_{\boldsymbol{\lambda}} \text{ is not calibrated} \quad (12)$$

Since the number of possible convex combinations is infinite, one cannot resort to standard ways for addressing multiple hypothesis testing problems, such as Bonferroni-correction or the Holm-Bonferroni method. In what follows, we will adopt the extreme value approach for high-dimensional testing [Dickhaus, 2015]. As a crucial observation, all individual tests are not independent, because only one member in $\mathcal{S}(\mathbf{x}, \mathcal{P})$ can correspond to the ground-truth $p(Y \mid \mathbf{x})$. Therefore, one can order all candidates in $\mathcal{S}(\mathbf{x}, \mathcal{P})$ from most likely to be $p(Y \mid \mathbf{x})$ to least likely to be $p(Y \mid \mathbf{x})$. All calibration measures considered in Section 2 are in essence decreasing functions of the *degree of calibration* of a probabilistic model, so one can simply search for the minimum of any calibration measure of interest over $\boldsymbol{\lambda} \in \Delta_M$. Then, the multiple hypothesis testing problem in (11) can be addressed by considering the distribution of the minimum under the null hypothesis.

Algorithm 1 Calibration Test for Credal Sets – **input:** $\mathcal{P}, \mathcal{D}_{\text{val}}, g, \alpha, D$

- 1: **for** $d = 1, \dots, D$ **do**
 - 2: $\mathcal{D}_d \leftarrow$ extract bootstrap sample of size N from \mathcal{D}_{val} (only features are further used)
 - 3: Sample uniformly $\lambda_{0,d} \in \Delta_M$
 - 4: For all $\mathbf{x}_i \in \mathcal{D}_d$, sample y_i from $\text{Cat}(\hat{\mathbf{p}}_{\lambda_{0,d}}(\mathbf{x}_i))$
 - 5: $t_{0d} \leftarrow g(\hat{\mathbf{p}}_{\lambda_{0,d}}, \mathcal{D}_d)$ $\triangleright g$ represents an arbitrary calibration measure
 - 6: $q_{1-\alpha} \leftarrow$ compute $(1 - \alpha)$ -quantile of empirical distribution $\{t_{0,1}, \dots, t_{0,D}\}$
 - 7: $t \leftarrow \min_{\lambda \in \Delta_M} g(\hat{\mathbf{p}}_{\lambda}, \mathcal{D}_{\text{val}})$ \triangleright Use an appropriate optimization algorithm for g
 - 8: reject H_0 if $t > q_{1-\alpha}$ and don't reject H_0 otherwise
-

This principle leads to a nonparametric test that is in fact a direct generalization of the test of Vaicnavicius et al. [2019]. The pseudocode of this procedure is given in Alg. 1. Starting from a set \mathcal{P} containing M fitted probabilistic models, a validation dataset $\mathcal{D}_{\text{val}} = \{(\mathbf{x}_1, y_1), \dots, (\mathbf{x}_N, y_N)\}$, and a general calibration measure g , such as HL_{cwise} or ECE_{conf} , the method first constructs the distribution of the calibration measure under the null hypothesis. To this end, it performs in total D runs with D a hyperparameter that trades off runtime versus p-value precision. In each run, a bootstrap sample of size N is sampled from the original validation dataset (line 2). Then, one $\lambda \in \Delta_M$ is selected at random and the corresponding element of the credal set $S(\mathbf{x}, \mathcal{P})$ is chosen as the ground-truth probability distribution, since we are working under the assumption that the null hypothesis is true (line 3). We assume that every element of $S(\mathbf{x}, \mathcal{P})$ is equally likely to correspond to the ground-truth distribution P , thus a uniform sample is drawn. Subsequently, for every instance in the bootstrap replicate, a label is randomly drawn from the selected probability distribution (line 4). In the last step of every run, the calibration measure is computed for the generated artificial labels and the ground-truth probability distribution (line 5). After D runs, we assume that a good estimate of the distribution of the calibration measure is obtained, under the assumption that the null hypothesis is true. Given a controlled Type I error rate α , the $(1 - \alpha)$ -quantile of this distribution is computed (line 6). This quantile defines the maximum allowed value of the calibration measure to accept the null hypothesis. Subsequently, the minimum of the calibration measure is computed for all members of the credal set, using now the original validation dataset (line 7). The null hypothesis is rejected if this minimum exceeds the threshold that was found under the empirical null distribution (line 8).

Two lines in the algorithm deserve some more discussion. In line 5, we compute the minimum of the calibration measure without solving an optimization problem. This is because we know the ground-truth probability distribution in this case. In the limit, when the sample size grows to infinity, the calibration measure g will even be zero, so in fact we are looking for the natural deviation from zero for a sample of size N .

Conversely, in line 7, we have to solve an optimization problem to find the minimum over $\lambda \in \Delta_M$. Specific solvers are needed here, because the objective functions are in most cases not differentiable, e.g., for the measures in (2), (4) and (5) this is not the case. The objective functions constructed from (6) and (7) are differentiable, but not convex. In this work we use constrained optimization by linear approximation (COBYLA), which is a numerical optimization method for constrained problems where the derivative of the objective function is not known [Powell, 1994]. In principle, any constrained derivative-free optimization algorithm can be used in line 7, and exploring other solvers will be considered in future work.

4 Experiments

Two types of experiments are considered in this work. First, we analyse the empirical Type I and II error of our statistical test for synthetic datasets. Second, we apply our test on several real-world datasets and popular ensemble-based credal predictors to investigate whether these methods return calibrated representations. Detailed information regarding the experimental setup and datasets can be found in App. A.

4.1 Type I and II error analysis

In a first set of experiments, we analyse the empirical Type I and II error rate for Alg. 1, with number of bootstrap samples $D = 100$, where we consider the calibration measures that have been discussed

in Section 2: $SKCE_{ul}$, HL_{cwise} , ECE_{conf} and ECE_{cwise} . For computational reasons, we choose not to incorporate $SKCE_{uq}$. For simplicity, we use a bin size of $B = 5$ and $B = 10$ for HL_{cwise} and $ECE_{conf,cwise}$. Similar as in Widmann et al. [2019], for $SKCE_{ul}$, we use the matrix-valued kernel $\Gamma(\mathbf{p}, \mathbf{p}') = \exp(-\|\mathbf{p} - \mathbf{p}'\|/2)\mathbf{I}_K$, combining the commonly-used total variation distance and the $K \times K$ identity matrix \mathbf{I}_K . Moreover, we analyse the statistical Type I and II error under three different scenarios, which we denote by S1, S2 and S3, respectively. S1 generates data under the null hypothesis that the credal predictor is calibrated, whereas S2 and S3 generate data under the alternative hypothesis that the credal predictor is not calibrated. To this end, we construct $R = 1000$ synthetic datasets that contain $N = 100$ instances. For each instance, we generate predictions for M probabilistic models and a ground-truth label: $\{(\mathbf{p}^{(1)}(\mathbf{X}_i), \dots, \mathbf{p}^{(M)}(\mathbf{X}_i), Y_i)\}_{i=1}^N$, with ensemble size $M = 10$, for $K = 10$ classes. For each dataset, we assume a mean $\mathbf{p}_e | \mathbf{X}_i \sim Dir(\mathbf{a}_e)$, with $a_{ek} = 1/K$ for all $k = 1, \dots, K$, and sample an ensemble from the prior $\mathbf{p}^{(1)}, \dots, \mathbf{p}^{(M)} | \mathbf{X}_i \sim Dir(K\mathbf{p}_e/u)$. By means of this prior, we are able to control the center \mathbf{p}_e and uncertainty (or spread) u of the credal sets, similarly as in [Sensoy et al., 2018a]. Then, we simulate the corresponding labels Y_i conditionally on the credal set in three ways:

- S1: The null hypothesis is true. For each dataset, we sample uniformly at random $\lambda \in \Delta_M$, and select \mathbf{p}_λ as the ground-truth probability distribution. We generate labels according to $Cat(\mathbf{p}_\lambda)$.
- S2: The null hypothesis is false. For each dataset, we generate labels using a categorical distribution that is randomly chosen outside the credal set on the line segment between the closest corner in Δ^K and \mathbf{p}_e .
- S3: The null hypothesis is false, too. Similarly as in S2, a categorical distribution is randomly chosen outside the credal set, but this time on the line segment between a randomly chosen corner in Δ^K and \mathbf{p}_e . In this case, it should be somewhat easier to reject the null hypothesis than in scenario S2.

The three different scenarios are illustrated in Fig. 1 (left) for $K = 3$ and $M = 10$. For scenarios S2 and S3, an additional algorithm is needed to compute the line segment outside the credal set. This algorithm is explained in App. A.1.

The results are shown in Fig. 1 (right). It appears that our test with $SKCE_{ul}$ leads to an empirical test error that is not upper bounded by the significance level, which makes our test with the calibration measure $SKCE_{ul}$ unreliable. Concerning the other measures, our test seems to be more conservative, in the sense that the Type I error is mostly lower than the significance level. HL_{cwise} does not seem to yield high power for S2, for different bin sizes. Empirically, our test with $ECE_{conf,cwise}$ results in reliable tests when it comes to both the Type I and Type II error. In App. B, we also show some results obtained for $u = 0.1$ (Fig. 2), $M = 100$ (Fig. 3) and $K = 100$ (Fig. 4). Similar findings are obtained w.r.t. the calibration measure $SKCE_{ul}$. For most cases, larger credal sets result in more conservative tests, as can be observed in Fig. 2. Increasing the ensemble size, however, does not seem to have a significant influence on the results, following Fig. 3. Finally, when looking at Fig. 4, when increasing the number of classes, the empirical test error approaches the significance level, and hence, making most tests less conservative.

4.2 Calibration of credal predictors based on deep neural networks

In a last set of experiments, we apply our test in Alg. 1 on six benchmark datasets, where we consider a single classifier (S) and three ensemble-based credal predictors: two dropout networks with rate 0.1 and 0.6 (DN(0.1), DN(0.6)) and a deep ensemble (DE), where we use an ensemble size of ten. For the deep ensembles, a credal predictor is obtained by training ten different models, i.e., with different initializations of the weights [Lakshminarayanan et al., 2017]. For the dropout networks, a credal predictor is obtained by using dropout in the last layer and sampling ten predictions [Gal, 2016]. For the image datasets, we consider a small and large neural network architecture that are commonly used in the literature: MobileNetV2 (MOB) with 3.4×10^6 parameters and VGG16 (VGG) with 138×10^6 parameters, respectively [Sandler et al., 2018, Simonyan and Zisserman, 2014]. For the last two biological datasets, a simple neural network with one hidden layer is considered, together with textual feature representations. For more information related to the training of the models and datasets, we refer the reader to App. A.2. Furthermore, we analyse the calibration of the credal predictors by means of the ECE_{conf} and ECE_{cwise} calibration measures, since those measures gave reliable tests in terms of Type I and Type II error in the previous simulations.

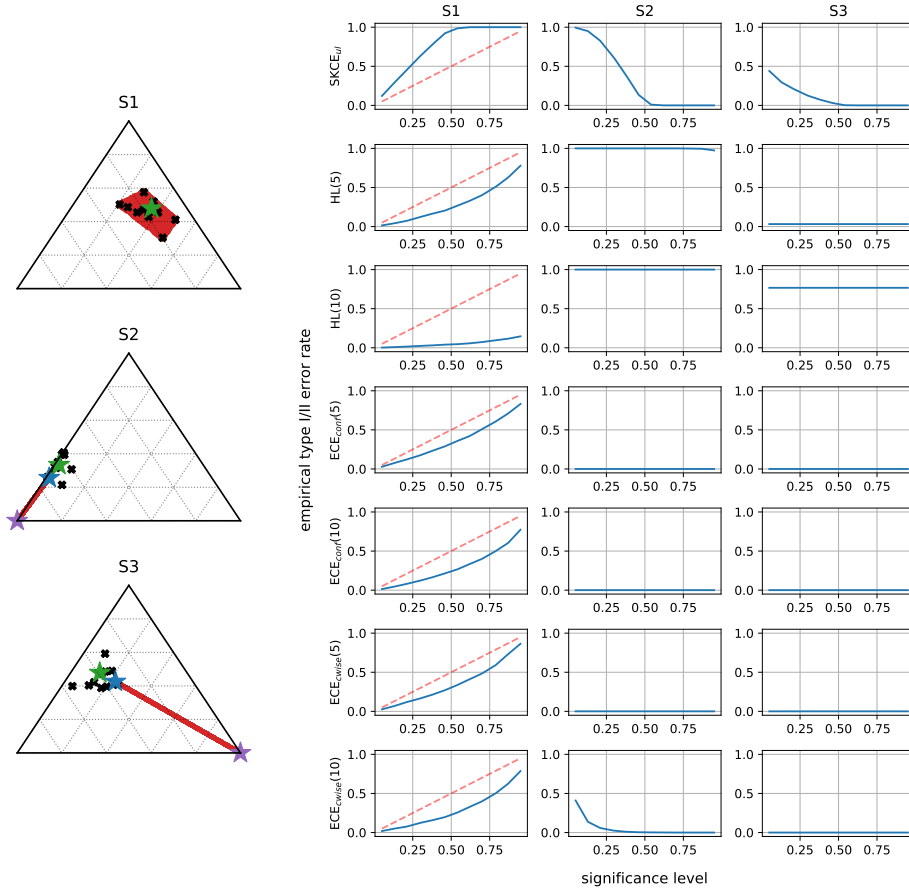


Figure 1: Left: A visualization of the setup in scenarios S1, S2 and S3. In all three scenarios, black stars correspond to an ensemble that has been sampled as outlined in the main text. In S1, the red dots correspond to a credal set from which the ground-truth distribution is uniformly sampled. In S2 and S3, the ground-truth distribution is uniformly sampled from the red line segment, outside the credal set. For S2, the line segment connects the calculated boundary (blue star) and closest corner in the simplex (purple star) of the credal set. For S3, the line segments connects a boundary of the credal set and a random corner in the simplex. Right: empirical Type I (S1) and Type II (S2, S3) error rate for different calibration measures in function of the significance level for $R = 1000$ randomly sampled datasets from S1, S2 and S3 and with $N = 100$, $M = 10$, $K = 10$ and $u = 0.01$. For all tests we use $D = 100$ bootstrap samples.

The results are shown in Table 1. For each predictor, we report results for the ensemble average, a setting which is often used in the literature that corresponds to taking the average of the ensemble predictions, and the weighted ensemble average, defined by λ that is obtained in line 7 of Alg. 1. More precisely, two different weighted ensemble averages are considered by running our test with the ECE_{conf} and ECE_{cwise} measure, respectively, on a specific calibration set. For each weighted average, we show the outcome of our test w.r.t. the set of hypotheses in (10), together with the average accuracy and calibration measure obtained on the test set. For the single classifier case, our test in Alg. 1 corresponds to the specific test from Vaicenavicius et al. [2019].

It is clear that single classifiers, based on deep neural networks, are in general not well-calibrated. This corresponds to similar findings that have been reported in literature [Guo et al., 2017]. For most cases, predictors are uncalibrated in terms of ECE_{cwise} , which is explained by the fact that class-wise calibration is a much stronger form of calibration. When it comes to ECE_{conf} and dropout networks, in some cases, our test does not reject the null hypothesis when a higher dropout rate is considered. This indicates that dropout networks tend to be better confidence calibrated, when using a higher dropout rate. This result is also confirmed by comparing the average ECE_{conf} on the test

Table 1: Results obtained for four different predictors: single classifier (S), dropout network with rate 0.1 (DN(0.1)) and 0.6 (DN(0.6)) and a deep ensemble (DE). Predictors are tested on six benchmark datasets. For the image datasets, we use two different architectures: VGG16 (VGG) and MobileNetV2 (MOB). For each predictor we consider the average and two different weighted averages, defined by the convex combination found in line 7 of Alg. 1, for ECE_{conf} and ECE_{cwise} , respectively. We report the average accuracy (Acc.) and calibration measure ($ECE_{conf,cwise}$) obtained on the test sets and report the outcome of our test for the different weighted averages on a separate calibration set.

DATASET	ARCH.	PREDICTOR	AVG.			WEIGHTED AVG.					
			ACC.	ECE_{conf}	ECE_{cwise}	REJ. H_0	λ_{conf} ACC.	ECE_{conf}	REJ. H_0	λ_{cwise} ACC.	ECE_{cwise}
CIFAR-10	MOB	S	0.7804	0.0194	0.0071	True	0.7804	0.0194	True	0.7804	0.0071
		DN(0.1)	0.7740	0.0612	0.0134	True	0.7726	0.0629	True	0.7730	0.0137
		DN(0.6)	0.3039	0.0196	0.0108	False	0.3025	0.0142	True	0.3007	0.0111
		DE	0.8329	0.1680	0.0327	False	0.7642	0.0150	True	0.7668	0.0062
	VGG	S	0.8438	0.0828	0.0183	True	0.8438	0.0828	True	0.8438	0.0183
		DN(0.1)	0.8476	0.0821	0.0183	True	0.8474	0.0832	True	0.8462	0.0181
		DN(0.6)	0.8355	0.0950	0.0202	True	0.8353	0.0954	True	0.8351	0.0203
		DE	0.8754	0.0044	0.0042	False	0.8756	0.0052	False	0.8766	0.0044
CALTECH-101	MOB	S	0.9477	0.0135	0.0010	True	0.9477	0.0135	True	0.9477	0.0010
		DN(0.1)	0.9384	0.0081	0.0010	False	0.9389	0.0087	True	0.9361	0.0010
		DN(0.6)	0.9338	0.0129	0.0012	False	0.9338	0.0107	True	0.9324	0.0012
		DE	0.9625	0.0175	0.0009	False	0.9509	0.0076	False	0.9579	0.0009
	VGG	S	0.9287	0.0395	0.0013	True	0.9287	0.0395	True	0.9287	0.0013
		DN(0.1)	0.9218	0.0192	0.0013	False	0.9204	0.0212	True	0.9218	0.0014
		DN(0.6)	0.9259	0.0155	0.0015	False	0.9162	0.0062	True	0.9157	0.0015
		DE	0.9500	0.0231	0.0011	False	0.9329	0.0079	False	0.9306	0.0011
CALTECH-256	MOB	S	0.7829	0.0638	0.0009	True	0.7829	0.0638	True	0.7829	0.0009
		DN(0.1)	0.7820	0.0473	0.0008	True	0.7816	0.0480	True	0.7823	0.0008
		DN(0.6)	0.7395	0.0201	0.0009	False	0.7313	0.0085	True	0.7336	0.0009
		DE	0.8383	0.0358	0.0007	False	0.8082	0.0130	True	0.8312	0.0006
	VGG	S	0.7552	0.0948	0.0011	True	0.7552	0.0948	True	0.7552	0.0011
		DN(0.1)	0.7458	0.0645	0.0011	True	0.7452	0.0663	True	0.7421	0.0011
		DN(0.6)	0.7427	0.0106	0.0010	False	0.7414	0.0103	True	0.7421	0.0010
		DE	0.8128	0.0326	0.0007	False	0.7864	0.0104	True	0.8108	0.0007
PLANTCLEF2015	MOB	S	0.4842	0.1300	0.0005	True	0.4842	0.1300	True	0.4842	0.0005
		DN(0.1)	0.4357	0.0866	0.0005	False	0.4320	0.0920	True	0.4319	0.0005
		DN(0.6)	0.4382	0.0199	0.0005	False	0.4343	0.0245	True	0.4348	0.0005
		DE	0.5973	0.0993	0.0004	False	0.5364	0.0171	True	0.5757	0.0004
	VGG	S	0.4085	0.1362	0.0006	True	0.4085	0.1362	True	0.4085	0.0006
		DN(0.1)	0.4156	0.1009	0.0006	False	0.4151	0.1020	True	0.4146	0.0006
		DN(0.6)	0.3927	0.0566	0.0005	False	0.3928	0.0566	True	0.3894	0.0005
		DE	0.5488	0.1045	0.0004	False	0.4705	0.0197	True	0.5236	0.0004
BACTERIA	-	S	0.8785	0.0507	0.0002	False	0.8785	0.0507	False	0.8785	0.0002
		DN(0.1)	0.8398	0.1504	0.0002	True	0.8345	0.1508	True	0.8371	0.0002
		DN(0.6)	0.8407	0.2085	0.0002	False	0.7491	0.0829	False	0.7879	0.0002
		DE	0.8926	0.1437	0.0002	False	0.8565	0.0642	False	0.9032	0.0001
PROTEINS	-	S	0.8001	0.0454	0.0001	True	0.8001	0.0454	True	0.8001	0.0001
		DN(0.1)	0.7909	0.0788	0.0001	True	0.7895	0.0779	True	0.7915	0.0001
		DN(0.6)	0.8117	0.0393	0.0001	True	0.8033	0.0353	True	0.8119	0.0001
		DE	0.8076	0.0764	0.0001	True	0.7968	0.0528	True	0.8050	0.0001

set between DN(0.1) and DN(0.6). A possible explanation could be given by the fact that the prior from which models are sampled in the dropout network with higher dropout rate, is more diverse and results in large credal sets that include the ground-truth distribution. Finally, when it comes to ECE_{conf} , deep ensembles appear to be calibrated for most datasets and architectures, since the null hypothesis is almost never rejected. For those predictors, there is also a significant difference in terms of ECE_{conf} between the average and weighted average, which indicates that using a simple averaging strategy results in less calibrated deep ensembles.

5 Discussion

In this paper we addressed the following question: What does it mean that a credal predictor represents epistemic uncertainty in a faithful manner? To answer this question, we referred to the notion of calibration of probabilistic predictors and extended it to credal predictors. We called a credal predictor calibrated if it returns sets that cover the true conditional probability distribution. To verify this property for the important case of ensemble-based credal predictors, we proposed a novel nonparametric calibration test that generalizes existing tests for probabilistic predictors to the case of credal predictors. In our experiments, we analyzed the Type I and II error of the newly-proposed

test for different scenarios. The best results were obtained when using expected calibration error as underlying calibration measure, but for most measures the Type I and II error were both sufficiently low. Making use of this test, we empirically show that credal classifiers based on deep neural networks are often not calibrated.

In future work, we would like to extend the statistical tests to other types of epistemic uncertainty representations. In this work, we are representing epistemic uncertainty on the level of models, i.e., probabilistic predictors $\hat{p} \in \mathcal{H}$, not on the level of (individual) predictions $\hat{p}(x)$. Therefore, we defined a credal set in (8) as a set containing all convex combinations of individual ensemble members. To capture predictive uncertainty, i.e., create a credal set on the level of individual predictions, one would need to generalize (8) to the case where λ may depend on x , i.e., is a function $\lambda(x) : \mathcal{X} \rightarrow \Delta_M$. To define and evaluate calibration in such a setting, a quite different statistical approach will be needed.

References

- T. Abe, E. K. Buchanan, G. Pleiss, R. Zemel, and J. P. Cunningham. Deep ensembles work, but are they necessary?, 2022.
- A. Amini, W. Schwarting, A. Soleimany, and D. Rus. Deep evidential regression. In *Advances in Neural Information Processing Systems*, volume 33, pages 14927–14937. Curran Associates, Inc., 2020.
- V. Bengs, E. Hüllermeier, and W. Waegeman. On the difficulty of epistemic uncertainty quantification in machine learning: The case of direct uncertainty estimation through loss minimisation, 2022.
- B. Charpentier, D. Zügner, and S. Günnemann. Posterior network: Uncertainty estimation without OOD samples via density-based pseudo-counts. In *Proc. NeurIPS, Neural Information Processing Systems*, 2020.
- G. Corani and A. Antonucci. Credal ensembles of classifiers. *Computational Statistics & Data Analysis*, 71:818–831, 2014. ISSN 0167-9473.
- J. Deng, W. Dong, R. Socher, L. Li, K. Li, and L. Fei-Fei. Imagenet: A large-scale hierarchical image database. In *IEEE CVPR*, pages 248–255, 2009.
- S. Depeweg, J.M. Hernandez-Lobato, F. Doshi-Velez, and S. Udfluft. Decomposition of uncertainty in Bayesian deep learning for efficient and risk-sensitive learning. In *Proc. ICML, 35th Int. Conf. on Machine Learning*, 2018.
- N. Dewolf, B. De Baets, and W. Waegeman. Valid prediction intervals for regression problems, 2021.
- T. Dickhaus. Simultaneous test procedures in high dimensions: the extreme value approach. In *International Conference on Computational Mathematics, Computational Geometry and Statistics*, 2015.
- M. Fagerland, D. Hosmer, and A. Bofin. Multinomial goodness-of-fit tests for logistic regression models. *Statistics in Medicine*, 27(12):4238–4253, 2008.
- A. Fiannaca, L. La Paglia, M. La Rosa, G. Lo Bosco, G. Renda, R. Rizzo, S. Gaglio, and A. Urso. Deep learning models for bacteria taxonomic classification of metagenomic data. *BMC Bioinformatics*, 19-S(7):61–76, 2018.
- T. S. Filho, H. Song, M. Perelló-Nieto, R. Santos-Rodríguez, M. Kull, and P. A. Flach. Classifier calibration: How to assess and improve predicted class probabilities: a survey. *CoRR*, abs/2112.10327, 2021.
- Y. Gal. *Uncertainty in Deep Learning*. PhD thesis, University of Cambridge, 2016.
- H. Goëau, P. Bonnet, and A. Joly. Lifeclef plant identification task 2015. In *Working Notes of CLEF 2015*, volume 1391, 2015.
- G. Griffin, A. Holub, and P. Perona. Caltech-256 object category dataset. Technical Report 7694, California Institute of Technology, 2007.

- C. Guo, G. Pleiss, Y. Sun, and K. Q. Weinberger. On calibration of modern neural networks. In *ICML*, volume 70 of *Proceedings of Machine Learning Research*, pages 1321–1330, 2017.
- S.C. Hora. Aleatory and epistemic uncertainty in probability elicitation with an example from hazardous waste management. *Reliability Engineering and System Safety*, 54(2–3):217–223, 1996.
- D. Hosmer and S. Lemeshow. *Applied Logistic Regression*. Wiley, 2003.
- E. Hüllermeier and W. Waegeman. Aleatoric and epistemic uncertainty in machine learning: An introduction to concepts and methods. *Machine Learning*, 110(3):457–506, 2021.
- A. Kendall and Y. Gal. What uncertainties do we need in Bayesian deep learning for computer vision? In *Proc. NIPS, Advances in Neural Information Processing Systems*, pages 5574–5584, 2017.
- A. Kathrin Kopetzki, B. Charpentier, D. Zügner, S. Giri, and S. Günnemann. Evaluating robustness of predictive uncertainty estimation: Are dirichlet-based models reliable? In *Proceedings of the 38th International Conference on Machine Learning, ICML*, pages 5707–5718, 2021.
- A. Krizhevsky, V. Nair, and G. Hinton. Cifar-10 (canadian institute for advanced research). Technical report, Canadian Institute for Advanced Research, 2010.
- B. Lakshminarayanan, A. Pritzel, and C. Blundell. Simple and scalable predictive uncertainty estimation using deep ensembles. In *Advances in Neural Information Processing Systems 30: Annual Conference on Neural Information Processing Systems*, pages 6402–6413, 2017.
- F. Li, M. Andreetto, and M. A. Ranzato. Caltech101 image dataset. Technical report, California Institute of Technology, 2003.
- Y. Li, S. Wang, R. Umarov, and et al. Deepre: sequence-based enzyme EC number prediction by deep learning. *BMC Bioinformatics*, 34(5):760–769, 2018.
- A. Malinin and M. Gales. Predictive uncertainty estimation via prior networks. In *Advances in Neural Information Processing Systems 31: Annual Conference on Neural Information Processing Systems*, 2018.
- V. Nguyen, M. H. Shaker, and E. Hüllermeier. How to measure uncertainty in uncertainty sampling for active learning. *Mach. Learn.*, 111(1):89–122, 2022.
- Y. Ovadia, E. Fertig, J. Ren, Z. Nado, D. Sculley, S. Nowozin, J. V. Dillon, B. Lakshminarayanan, and J. Snoek. Can you trust your model’s uncertainty? evaluating predictive uncertainty under dataset shift. *Neurips*, 2019.
- A. Paszke, S. Gross, S. Chintala, and et al. Automatic differentiation in pytorch. In *NIPS-W*, 2017.
- M. J. D. Powell. *A Direct Search Optimization Method That Models the Objective and Constraint Functions by Linear Interpolation*, pages 51–67. Kluwer Academic, 1994.
- RIKEN. Genomic-based 16s ribosomal rna database, 04 2013. URL <https://metasystems.riken.jp/grd/download.html>.
- M. Sandler, A. Howard, M. Zhu, A. Zhmoginov, and L. Chen. Mobilenetv2: Inverted residuals and linear bottlenecks, 2018.
- R. Senge, S. Bösner, K. Dembczynski, J. Haasenritter, O. Hirsch, N. Donner-Banzhoff, and E. Hüllermeier. Reliable classification: Learning classifiers that distinguish aleatoric and epistemic uncertainty. *Information Sciences*, 255:16–29, 2014.
- M. Sensoy, L. Kaplan, and M. Kandemir. Evidential deep learning to quantify classification uncertainty. In *Advances in Neural Information Processing Systems*, volume 31. Curran Associates, Inc., 2018a.
- M. Sensoy, L. Kaplan, and M. Kandemir. Evidential deep learning to quantify classification uncertainty. In *Proc. NeurIPS, 32nd Conf. on Neural Information Processing Systems*, 2018b.

- M.H. Shaker and E. Hüllermeier. Aleatoric and epistemic uncertainty with random forests. In *Proc. IDA, 18th Int. Symposium on Intelligent Data Analysis*, volume 12080 of *LNCS*, pages 444–456, Konstanz, Germany, 2020. Springer.
- K. Simonyan and A. Zisserman. Very deep convolutional networks for large-scale image recognition. *CoRR*, abs/1409.1556, 2014.
- J. Vaicenavicius, D. Widmann, C. R. Andersson, F. Lindsten, J. Roll, and T.̄. Schön. Evaluating model calibration in classification. In *The 22nd International Conference on Artificial Intelligence and Statistics, AISTATS*, volume 89 of *Proceedings of Machine Learning Research*, pages 3459–3467. PMLR, 2019.
- P. Walley. *Statistical Reasoning with Imprecise Probabilities*. Chapman and Hall, 1991.
- D. Widmann, F. Lindsten, and D. Zachariah. Calibration tests in multi-class classification: A unifying framework. In *Advances in Neural Information Processing Systems 32: Annual Conference on Neural Information Processing Systems*, pages 12236–12246, 2019.
- G. Yang, S. Destercke, and M. Masson. Nested dichotomies with probability sets for multi-class classification. In *ECAI*, pages 363–368, 2014.
- B. Zadrozny and C. Elkan. Obtaining calibrated probability estimates from decision trees and naive bayesian classifiers. In *ICML*, pages 609–616, 2001.

A Experimental setup

A.1 Type I and II error analysis

Here we explain in detail how the ground-truth distribution is generated in scenarios S2 and S3. In both cases, the null hypothesis is false, so one needs to sample a ground-truth distribution outside the credal set. To find a distribution outside the credal set, for every \mathbf{x} , we need to find the largest $\lambda_b \in [0, 1]$, such that $\mathbf{p}_{\lambda_b} \in S(\mathbf{x}, \mathcal{P})$, with $\mathbf{p}_{\lambda_b} = (1 - \lambda_b)\mathbf{p}_e + \lambda_b\mathbf{p}_c$, \mathbf{p}_e the mean and \mathbf{p}_c the randomly chosen corner. This can be calculated by means of an exhaustive line search for λ over the interval $[0, 1]$ and a linear program. Pseudocode for this procedure is given by Alg. 2. After finding the boundary, one can simply sample a random distribution on the line segment between \mathbf{p}_{λ_b} and \mathbf{p}_c .

Algorithm 2 findBoundary – **input:** $S(\mathbf{x}, \mathcal{P})$, \mathbf{p}_0 , \mathbf{p}_c , LP

```

1:  $\mathbf{P} \leftarrow [\mathbf{p}^{(1)}; \dots; \mathbf{p}^{(M)}]$ , i.e.,  $\mathbf{P} \in [0, 1]^{M \times K}$  ▷  $\mathbf{P}$  represents  $\mathcal{P}$  in matrix-notation
2:  $\mathbf{A} = [\mathbf{P}^T; \mathbf{1}_M]$  with row vector  $\mathbf{1}_M = [1, \dots, 1]$ 
3:  $\mathbf{p}_{\lambda_b} \leftarrow \mathbf{p}_0$ 
4: for  $\lambda' = 0$  to 1 do ▷ Begin exhaustive line search
5:    $\mathbf{p}_{\lambda'} \leftarrow (1 - \lambda')\mathbf{p}_0 + \lambda'\mathbf{p}_c$ 
6:    $\mathbf{z} = [\mathbf{p}_{\lambda'}; 1]$ 
7:   if LP( $\mathbf{A}, \mathbf{z}$ ) finds a solution then ▷ Check if  $\mathbf{p}_{\lambda'}$  falls inside the credal set
8:      $\mathbf{p}_{\lambda_b} \leftarrow \mathbf{p}_{\lambda'}$ 
9:   else
10:    break ▷ We are outside the credal set, hence, break and return previous solution
11: return  $\mathbf{p}_{\lambda_b}$ 

```

A.2 Calibration of credal predictors based on deep neural networks

We use a MobileNetV2 or VGG16 convolutional neural network [Sandler et al., 2018, Simonyan and Zisserman, 2014], pretrained on ImageNet [Deng et al., 2009], in order to obtain hidden representations for all image datasets. For the bacteria dataset, tf-idf representations are obtained by means of extracting 3-, 4- and 5-grams from the 16S rRNA sequences that were provided in the dataset [Finnaca et al., 2018]. For the proteins dataset, tf-idf representations are obtained by considering 3-grams only. Furthermore, to comply with literature, the tf-idf representations are concatenated

Table 2: Overview of of image (top) and text (bottom) datasets used in the experiments. Notation: K – number of classes, D – number of features, N – number of samples for training, calibration and test set.

Dataset	K	D	N_{train}	$N_{\text{cal.}}$	N_{test}
CIFAR-10 [Krizhevsky et al., 2010]	10	1000	50000	4992	4992
Caltech-101 [Li et al., 2003]	97	1000	4338	2160	2160
Caltech-256 [Griffin et al., 2007]	256	1000	14890	7440	7440
PlantCLEF2015 [Goëau et al., 2015]	1000	1000	91758	10720	10720
Bacteria [RIKEN, 2013]	2659	1000	10587	1136	1136
Proteins [Li et al., 2018]	3485	1000	11830	5088	5088

with functional domain encodings, which contain distinct functional and evolutionary information about the protein sequence [Li et al., 2018]. Next, obtained feature representations for the biological datasets are passed through a single-layer neural net with 1000 output neurons and a ReLU activation function. We use the categorical cross-entropy loss by means of stochastic gradient descent with momentum, where the learning rate and momentum are set to $1e-5$ and 0.99, respectively. We set the number of epochs to 2 and 20, for the Caltech and other datasets, respectively. We train all models end-to-end on a GPU, by using the PyTorch library [Paszke et al., 2017] and infrastructure with the following specifications:

- **CPU:** i7-6800K 3.4 GHz (3.8 GHz Turbo Boost) – 6 cores / 12 threads,
- **GPU:** 2x Nvidia GTX 1080 Ti 11GB + 1x Nvidia Tesla K40c 11GB,
- **RAM:** 64GB DDR4-2666.

B Additional experiments

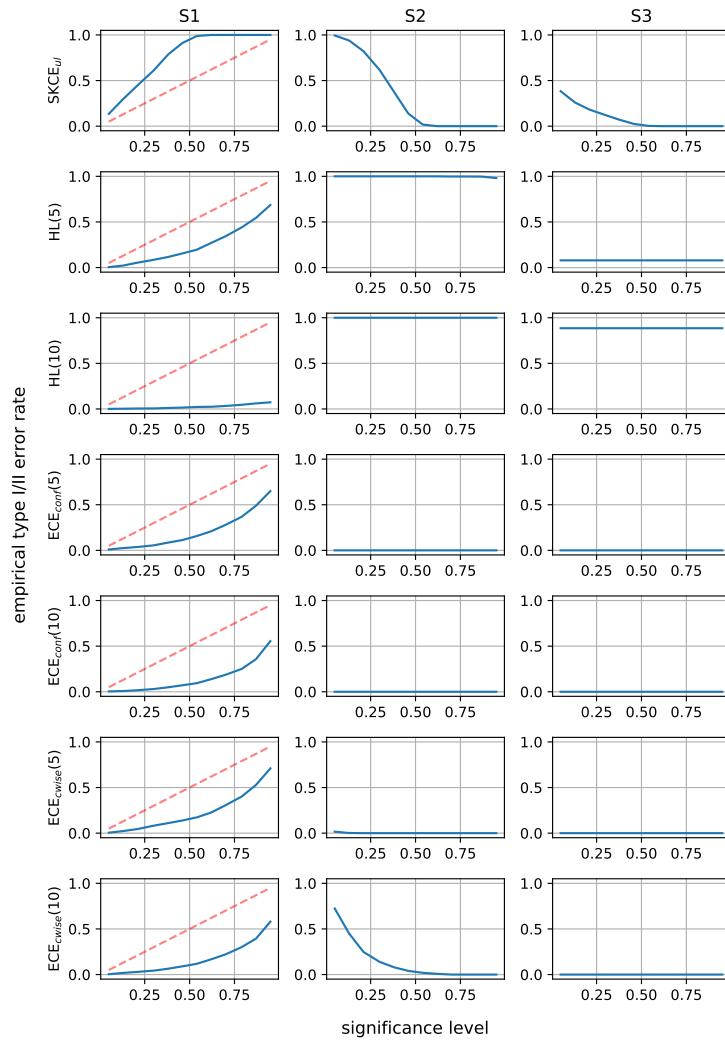


Figure 2: Empirical Type I (S1) and Type II (S2, S3) error for different calibration measures in function of the significance level for $R = 1000$ randomly sampled datasets from S1, S2 and S3 and with $N = 100, M = 10, K = 10$ and $u = 0.1$. For all tests we use $D = 100$ bootstrap samples.

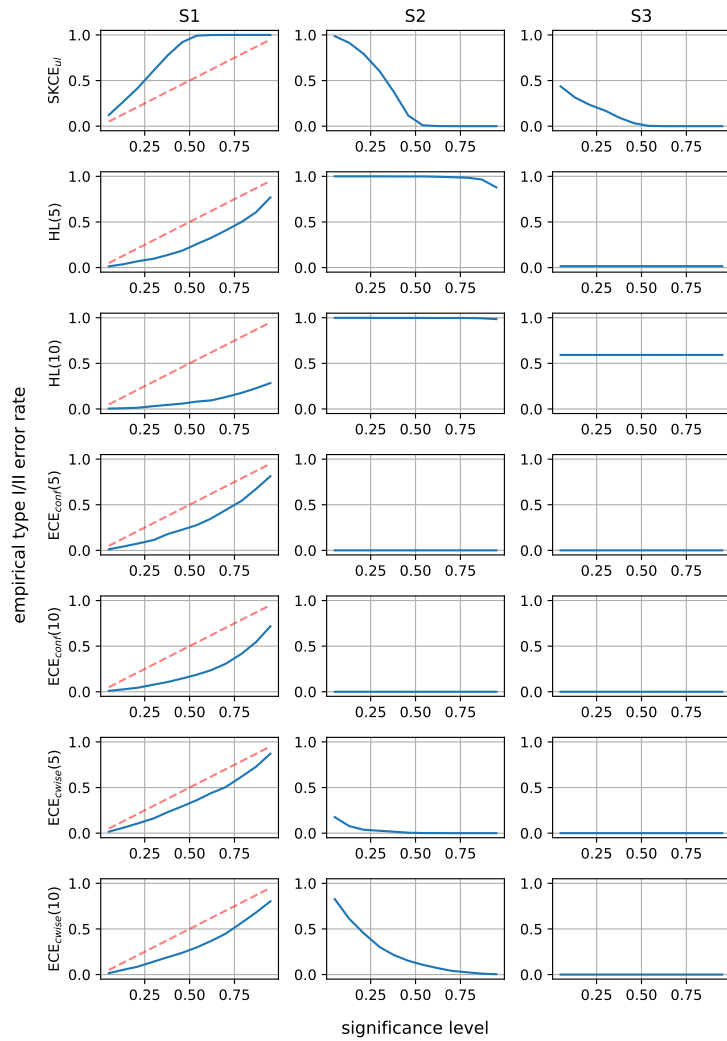


Figure 3: Empirical Type I (S1) and Type II (S2, S3) error for different calibration measures in function of the significance level for $R = 1000$ randomly sampled datasets from S1, S2 and S3 and with $N = 100, M = 100, K = 10$ and $u = 0.01$. For all tests we use $D = 100$ bootstrap samples.

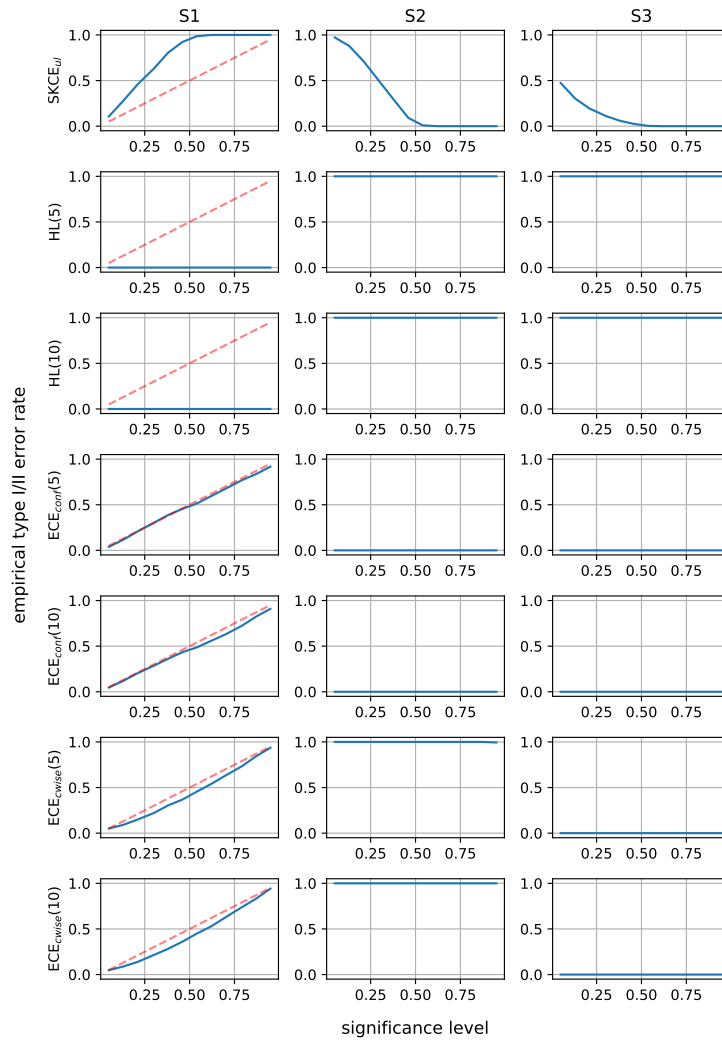


Figure 4: Empirical Type I (S1) and Type II (S2, S3) error for different calibration measures in function of the significance level for $R = 1000$ randomly sampled datasets from S1, S2 and S3 and with $N = 100$, $M = 10$, $K = 100$ and $u = 0.01$. For all tests we use $D = 100$ bootstrap samples.